An Orientation-based Random Waypoint Model for User Mobility in Wireless Networks

Mohammad Dehghani Soltani, Ardimas Andi Purwita, Zhihong Zeng, Cheng Chen, Harald Haas, and Majid Safari
LiFi Research and Development Centre, School of Engineering, University of Edinburgh, Edinburgh, UK
emails: {m.dehghani, a.purwita, zhihong.zeng, cheng.chen, h.haas, majid.safari}@ed.ac.uk

***Abstract*—In the context of optical wireless communications (as well as millimeter wave and terahertz systems), it is important to consider the random orientation of the user equipment (UE). At such small wavelengths, the UE's random orientation affects the angle of arrival or incidence angle that leads to a change in channel gain as well as the received signal-to-noise ratio (SNR). Furthermore, it can result in frequent handover that may affect user's quality of experience. Hence, it is required to consider the random orientation of the UE in our analysis to obtain more realistic results. Therefore, a framework that combines the conventional mobility models with the random orientation model is required. In this study, we propose an extended orientation-based random waypoint mobility model, in which the random orientation of the UE is considered during both walking and pause time. The parameters of the model are set based on the experimental measurements of device orientation. The application of this model to an indoor light-fidelity (LiFi) network is studied as a use case by analyzing the handover rate.**

***Index Terms*—Mobility, random waypoint, random orientation, LiFi.**

I. Introduction

High-frequency (above 30 GHz) radio frequency (RF) communication technologies such as millimeter wave (30 to 300 GHz), terahertz (300 GHz to 3 THz) and optical wireless communications (10 THz to 1 PHz), are highly sensitive to a change in location and orientation of devices, see [1]–[3]. These technologies are possible candidates for next generations of wireless communications with much higher data rate requirements [4]. However, to be integrated in future generations of cellular networks, system-level design as well as network-level analyses of these networks are required by means of more realistic models for mobility and orientation.

A frequently-used mobility model for wireless cellular networks is the random waypoint (RWP) model [5]–[9]. The RWP provides flexibility, such as the incorporation of occasional pause times in modeling the mobility of users. However, the conventional RWP is not a complete model for light-fidelity (LiFi) and millimeter wave (mmWave) cellular networks. The reason behind this is that it does not consider the random orientation of the user equipment (UE). In fact, in both LiFi and mmWave networks, the random orientation of the UE is an important factor since a change in the device orientation affects the UE's performance. For instance, it can lead to a handover that would not normally happen in conventional RF systems. Hence, it is crucial to incorporate the random orientation of the UE with user mobility to provide a more realistic framework for the performance analysis in LiFi and mmWave networks.

In our recent studies, we derived the statistical models of device orientation for sitting and walking activities by recording instantaneous rotation angles of smartphones [10]–[13]. The statistical results are obtained based on experimental measurements for three elemental rotation angles called Euler angles. It is shown that these angles follow Laplace distributions for sitting activities while for walking activities they are well-fitted to Gaussian distributions [13]. Device orientation has also been analyzed from a temporal point of view [10], [14]. The recorded experimental data confirms that the measured rotation angles are correlated [13]. Hence, methods to generate a correlated Gaussian random process (RP) based on the first-order autoregressive (AR) model [10], [13] and harmonic RP [14] are proposed. In [10], a correlated Gaussian RP based on AR(1) is proposed for the polar angle and it is incorporated into the conventional RWP, which is called the orientation-based random waypoint (ORWP) mobility model. In [13], [15], the ORWP mobility model has been used for a receiver with multiple photodetectors (PDs) by modeling each elemental rotation angle as a Gaussian RP.

The above studies did not consider 'pause time' in their simulations. However, in a realistic mobility model the users may pause for random periods of time when users remain static [5]. Users are static during pause time. According to [10], the orientation model for static users follows a Laplace distribution, which is different from the one for walking activities, i.e., the Gaussian distribution. More importantly, random orientation may not be a stationary RP during the pause time, which has not been investigated in previous studies. In this study, the ORWP will be further extended to include the random orientation behavior of a UE during both movement and pause time as a correlated Gaussian RP and a correlated Laplace RP, respectively. Furthermore, the non-stationary behavior of random orientation during the pause time as well as the fluctuations about the azimuth angle have been considered to provide a more realistic framework for the analysis of mobility in optical wireless networks. The rest of this paper is organized as follows. In Section II, the system model is presented. The proposed ORWP is discussed in Section III. Simulation results are presented in Section IV. Section V concludes this paper.

978-1-7281-7440-2/20/$31.00 ©2020 IEEE

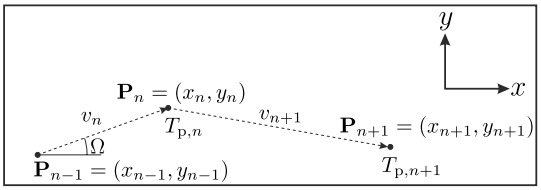

Fig. 1: Random waypoint mobility model.

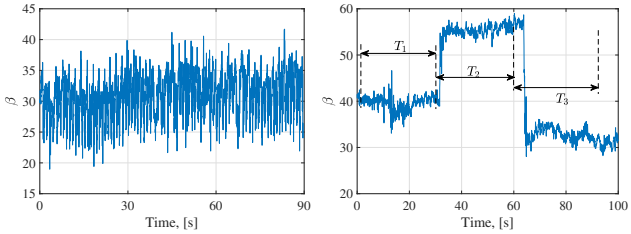

(a) (b)

Fig. 2: Realizations of β for (a) a walking user, (b) a static user.

II. System Model

A. LiFi Channel Model

The direct current (DC) gain of the line-of-sight (LoS) component of LiFi systems is given as [16]:

$$H = \frac{(m+1)A_{\mathrm{PD}}}{2\pi d^2}\cos^m\phi\; g_{\mathrm{f}}g(\psi)\cos\psi\;\mathrm{rect}\left(\frac{\psi}{\Psi_{\mathrm{c}}}\right), \quad (1)$$

where the area of the PD is denoted by A_{PD}, ψ and ϕ are the angle of incidence with respect to the axis normal to the receiver surface, and the angle of radiance with respect to the axis normal to the transmitter surface, respectively. The receiver field of view (FOV) is Ψ_{c}; and $\mathrm{rect}(\frac{\psi}{\Psi_{\mathrm{c}}}) = 1$ for $0 \le \psi \le \Psi_{\mathrm{c}}$ and 0 otherwise. The gain of the optical filter is shown by g_{f}. The optical concentrator, is given as $g(\psi) = \varsigma^2/\sin^2\Psi_{\mathrm{c}}$, if $0 \le \psi \le \Psi_{\mathrm{c}}$, otherwise $g(\psi) = 0$; where ς is the refractive index. In (1), m is the Lambertian order which is $m = -1/\log_2(\cos\Phi_{1/2})$, where $\Phi_{1/2}$ is the half-intensity angle. The radiance angle ϕ and the incidence angle ψ of the transmitter and the receiver can be calculated as:

$$\cos\phi = \frac{-\mathbf{d}\cdot\mathbf{n}_{\mathrm{t}}}{\|\mathbf{d}\|}, \qquad \cos\psi = \frac{\mathbf{d}\cdot\mathbf{n}'_{\mathrm{u}}}{\|\mathbf{d}\|}, \quad (2)$$

where $\mathbf{n}_{\mathrm{t}} = [0,0,-1]^{\mathrm{T}}$ and $\mathbf{n}'_{\mathrm{u}}$ are the normal vectors at the transmitter and the receiver planes, respectively and $\mathbf{d}$ is the distance vector from the receiver to the transmitter. The symbols $\cdot$ and $\|\cdot\|$ are the inner product and the Euclidean norm operators, respectively. Also $(.)^{\mathrm{T}}$ is the transpose operator.

B. Random Orientation Model

The UE orientation can be expressed by three elemental angles yaw, α, pitch, β, and roll, γ [17], which can be measured by various sensors mounted on a smartphone. Based on Euler's rotation theorem [18], the three elemental rotations can be described by three elemental rotation matrices, which are denoted as $\mathbf{R}_\alpha$, $\mathbf{R}_\beta$ and $\mathbf{R}_\gamma$, respectively. And the overall rotation matrix is denoted as $\mathbf{R} = \mathbf{R}_\alpha\mathbf{R}_\beta\mathbf{R}_\gamma$. The normal vector perpendicular to the screen of the smartphone is denoted as $\mathbf{n}_{\mathrm{u}} = [n_1, n_2, n_3]^{\mathrm{T}}$. The normal vector after rotation, $\mathbf{n}'_{\mathrm{u}} = [n'_1, n'_2, n'_3]^{\mathrm{T}}$, can be obtained as $\mathbf{n}'_{\mathrm{u}} = \mathbf{R}\mathbf{n}_{\mathrm{u}}$. The distribution of the random UE orientation (i.e., rotational angles) has been measured and modeled for both walking and sitting scenarios [10], [13]. It has been shown in [13] that the three angles α, β and γ follow a Gaussian or a Laplace distribution for walking or static users, respectively.

C. Conventional Random Waypoint Model

According to the RWP model, at each waypoint, the movement of the UE needs to follow three rules, i) users randomly choose their destinations in the room area; ii) users move straight from source to destination with a constant speed; iii) the users may pause for a random period of time at the destination before moving again. The RWP mobility model is described as a discrete-time stochastic process. Mathematically, the RWP can be denoted as an infinite sequence of quadruple: $\left\{(\mathbf{P}_{n-1}, \mathbf{P}_n, v_n, T_{\mathrm{p,n}}) \;\middle|\; n \in \mathbb{N}\right\}$ where n stands for the nth movement period. As shown in Fig. 1, the UE moves from the random waypoint $\mathbf{P}_{n-1} = (x_{n-1}, y_{n-1})$ to the destination point $\mathbf{P}_n = (x_n, y_n)$ with a speed of v_n chosen from a random distribution of f_v [5]. Then, it pauses at the destination for a period of $T_{\mathrm{p},n}$. The transition length is defined as $\mathcal{D}_n = \|\mathbf{P}_n - \mathbf{P}_{n-1}\|$, which is the Euclidean distance between two consecutive waypoints, $\mathbf{P}_{n-1}$ and $\mathbf{P}_n$. The angle between the direction of movement and the positive direction of the x-axis is defined as the angle of direction, Ω, as shown in Fig. 1. The elapsed time between two successive movements for the nth period is given as $T_{\mathrm{e},n} = T_{\mathrm{D},n} + T_{\mathrm{p},n}$, where $T_{\mathrm{D},n} = \mathcal{D}_n/v_n$ and $T_{\mathrm{p},n}$ denotes the pause time at the destination, which is chosen from a random distribution of $f_{T_{\mathrm{p}}}$. In this study, it is assumed that $f_{T_{\mathrm{p}}}$ is an exponential distribution with a mean value of $\mathbb{E}[T_{\mathrm{p}}]$ [5].

III. Extended Orientation-based Random Waypoint Model

In the context of LiFi as well as mmWave cellular networks, the effect of a UEs' orientation on the performance of the system is significant. In fact, a significant change of UEs' orientation, whether individually or combined with the mobility of the user, can lead to a handover that would not normally happen for UEs with a constant orientation. So in order to provide a realistic framework to analyze the performance of mobile wireless networks, we need to combine the conventional RWP with the random orientation of the UE.

However, in order to integrate the random orientation of a device with user mobility, it is required to model it as a RP. According to the experimental measurements [10], the elemental rotation angles, i.e. α, β and γ, can be modeled as stationary correlated Gaussian RPs for walking users. However, for static users, sudden changes are occasionally observed after random periods in these angles; hence, they can be modeled more realistically as non-stationary Laplace RPs [14]. One realization of β (obtained from experimental measurements) is shown in Fig. 2a for a mobile user and Fig. 2b for a static user. The correlated Gaussian and Laplace RP are described in the following subsections.

A. Correlated Gaussian Process

A simple method to generate a correlated Gaussian RP is to pass a white noise process through a linear time-invariant (LTI) filter, e.g., using a linear AR model. The goal is to match the generated RP to the moments and the coherence time of the elemental rotation angles measured experimentally. Hence, it is sufficient to only consider first-order AR model by assuming $p = 1$ to generate the correlated Gaussian RP. Therefore, after passing the white noise process, $w[n]$, through the LTI filter, the nth sample of the AR(1) model can be expressed as:

$$\alpha[n] = c_0 + c_1\alpha[n-1] + w[n], \tag{3}$$

where c_0 denotes the biased level and c_1 is a constant factor. To guarantee the RP, α, is wide-sense stationary, c_1 should meet the condition $|c_1| < 1$. The mean, variance and autocorrelation function (ACF) of AR(1) are denoted as [19]:

$$\mathbb{E}[\alpha] = \frac{c_0}{1-c_1}, \quad \sigma_\alpha^2 = \frac{\sigma_w^2}{1-c_1^2}, \quad \mathcal{R}_\alpha(\ell) = c_1^\ell, \tag{4}$$

where σ_w^2 is the variance of white noise RP, w. Note that the coherence time of RP α is denoted as $T_{\mathrm{c},\alpha}$ and defined as the time that satisfies $\mathcal{R}_\alpha(\ell_\alpha = \frac{T_{\mathrm{c},\alpha}}{T_\mathrm{s}}) = 0.05$, where T_s is the sample time. Based on the above equations, we have:

$$c_0 = (1-c_1)\mathbb{E}[\alpha], \quad \sigma_w^2 = (1-c_1^2)\sigma_\alpha^2, \quad c_1 = 0.05^{\frac{T_\mathrm{s}}{T_{\mathrm{c},\alpha}}}. \tag{5}$$

The nth time sample of the correlated Gaussian RP, α, can be determined according to (3) after determining the parameters of the AR(1) model. Using the same method, the nth sample of β and γ can also be specified.

B. Correlated Laplace Process

The experimental measurements illustrate that the mean value of β changes after a random period T_i, $i \in \mathbb{N}$, when users are static. This behavior is not observed in the experimental data of walking users which means that they tend to keep their smartphone with a constant mean value during the movement, however with some fluctuations around it (please see Fig. 2a and 2b). Therefore, the RP β is not stationary for static users. However, it is fair to assume it as a weak-sense stationary (WSS) RP over small duration of T_i. Hence, we aim to provide a new framework to model the non-stationary behavior of β by breaking it into small stationary RPs. We assume that T_i follows an exponential distribution with a mean value of T_m. It is also assumed that the mean value, $\overline{\beta}_i$, at each T_i are chosen randomly from a uniform distribution $\mathcal{U}(\overline{\beta}_{\min}, \overline{\beta}_{\max})$. Note that these two assumptions does not change the generality of the model and other distributions can be also assumed. Next, we need to create correlated Laplace samples with the mean and variance of $\overline{\beta}_i$ and $\hat{\sigma}^2_{\beta,i}$ for each duration of T_i.

Methods to generate a zero-mean Laplace process with a desired ACF is introduced in [20], [21]. The methods are based on the multiplication of independent zero-mean Gaussian RPs. We use a similar procedure to generate a non-zero correlated Laplace RP as shown in Fig. 3. That is, after passing the complex white noise, w_i, $i = 1, 2$, through an AR(1) LTI filter, the correlated Gaussian noise ϑ_1 and ϑ_2 are produced. The

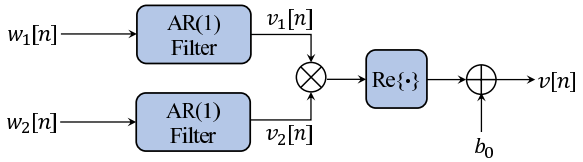

Fig. 3: Block diagram of generating the correlated Laplace process.

real or imaginary part of the multiplication of these correlated Gaussian noise, ϑ_1 and ϑ_2, is a correlated zero-mean Laplace process. Based on the desired mean value for the final RP, ϑ, the bias b_0 is added to it. Without loss of generality, we assume that the AR(1) filters have equal orders and they are identical. In this study and for the purpose of simplicity, we only considered the first-order autoregressive process, i.e., AR(1). In fact, as it will be shown in Lemma 1, this simple model is sufficient to match the mean, variance and the coherence time of the generated RP ϑ to the statistics of α, β and γ provided in Table I of [13].

Let $\vartheta_i[n]$ represents the nth sample of the correlated complex RP, ϑ_i, obtained from AR(1) model, then we have:

$$\vartheta_i[n] = c_0 + c_1\vartheta_i[n-1] + w[n], \quad i = 1, 2 \tag{6}$$

To ensure that ϑ_1 and ϑ_2 are zero-mean RPs, $c_0 = 0$. The parameters c_1, σ_w^2 and b_0 should be obtained in such a way that match the statistics of the correlated Laplace RP, ϑ. These parameters can be uniquely determined using the following lemma.

Lemma 1: The expected value, variance and ACF of the RP ϑ are given as:

$$\mathbb{E}[\vartheta] = b_0, \quad \sigma_\vartheta^2 = \frac{\sigma_w^4}{2(1-c_1^2)^2}, \quad \mathcal{R}_\vartheta(\ell) = c_1^{2\ell}. \tag{7}$$

Proof: See Appendix.

For the RP α, the parameter c_1 can be first determined by matching the coherence time of the RP to the one obtained from experimental measurements. Therefore, by substituting $\ell = \frac{T_{\mathrm{c},\alpha}}{T_\mathrm{s}}$ in (7) and noting that $\mathcal{R}_\alpha(\ell = \frac{T_{\mathrm{c},\alpha}}{T_\mathrm{s}}) = 0.05$ [22], we have:

$$c_1 = 0.05^{\frac{T_\mathrm{s}}{2T_{\mathrm{c},\alpha}}}. \tag{8}$$

From (7), we have:

$$\sigma_w^2 = \sqrt{2}\sigma_\vartheta(1-c_1^2). \tag{9}$$

Finally, the nth sample of the correlated Laplace process, α, is given as:

$$\alpha[n] = \mathrm{Re}\left\{\alpha_1[n]\alpha_2[n]\right\} + b_0, \tag{10}$$

where $\alpha_i[n] = c_1\alpha[n-1] + w[n]$ for $i = 1, 2$ and $\mathrm{Re}\{\cdot\}$ picks the real part. This approach can be repeated to obtain the correlated samples of the RPs β and γ. For the RP β the samples are determined based on the corresponding $\overline{\beta}_i$ and $\hat{\sigma}^2_{\beta,i}$ for each duration of T_i.

By combining the two methods described above in subsections A and B, one can readily generate samples of device orientation whether the user is mobile or static. Hence, the ORWP that incorporates the orientation with RWP mobility can be modeled as an infinite sequence of

Algorithm 1 Extended orientation-based random waypoint

Initialization:
Denote $\mathbf{P}_0=(x_0,y_0)$ as the initial UE's position
N as the number of simulation runs; v as the average speed of UE; $T_{\mathrm{c},\alpha}$, $T_{\mathrm{c},\beta}$ and $T_{\mathrm{c},\gamma}$ as the coherence time of α, β and γ, respectively; Set $T_{\mathrm{c}}=\min\{T_{\mathrm{c},\alpha},T_{\mathrm{c},\beta},T_{\mathrm{c},\gamma}\}$;
for $k=1:N$ **do**
  Choose a random position $\mathcal{P}_k=(x_k,y_k)$
  Compute $\mathcal{D}_k=\|\mathcal{P}_k-\mathcal{P}_{k-1}\|$
  Compute $\Omega=\tan^{-1}\left(\frac{y_k-y_{k-1}}{x_k-x_{k-1}}\right)$
  $t_{\mathrm{move}}\longleftarrow 0$
  $n\longleftarrow 1$;
  while $t_{\mathrm{move}}\leq\frac{\mathcal{D}_k}{v}$ **do**
    Compute $\mathbf{P}_n=(x_n,y_n)$ with $x_n=x_{n-1}+vT_{\mathrm{c}}\cos\Omega$ and $y_n=y_{n-1}+vT_{\mathrm{c}}\sin\Omega$
    Generate $\Theta_n=(\alpha_n,\beta_n,\gamma_n)$ based on the correlated Gaussian AR(1) model described in Section III-A
    Return $(\mathbf{P}_{n-1},\mathbf{P}_n,v,0,\Theta_n)$ as ORWP specifications
    $n\longleftarrow n+1$
    $t_{\mathrm{move}}\longleftarrow t_{\mathrm{move}}+T_{\mathrm{c}}$
  end while
  if $t_{\mathrm{move}}\neq\frac{\mathcal{D}_k}{v}-T_{\mathrm{c}}$ **then**
    Generate $\Theta_n=(\alpha_n,\beta_n,\gamma_n)$ based on the correlated Gaussian AR(1) model described in Section III-A
    $\mathbf{P}_n\longleftarrow\mathcal{P}_k$
    Return $(\mathbf{P}_{n-1},\mathbf{P}_n,v,0,\Theta_n)$ as ORWP specifications
    $n\longleftarrow n+1$
  end if
  Choose a random pause time $T_{\mathrm{p},n}$ from a random distribution of $f_{T_{\mathrm{p}}}$
  $t_{\mathrm{pause}}\longleftarrow 0$
  while $t_{\mathrm{pause}}\leq T_{\mathrm{p},n}+T_{\mathrm{c}}$ **do**
    Generate $\Theta_n=(\alpha_n,\beta_n,\gamma_n)$ based on the correlated Laplace AR(1) model described in Section III-B
    $\mathbf{P}_n\longleftarrow\mathbf{P}_{n-1}$
    Return $(\mathbf{P}_{n-1},\mathbf{P}_n,v,T_{\mathrm{p},n},\Theta_n)$ as ORWP specifications
    $n\longleftarrow n+1$
    $t_{\mathrm{pause}}\longleftarrow t_{\mathrm{pause}}+T_{\mathrm{c}}$
  end while
  $k\longleftarrow k+1$
end for

$\big\{(\mathbf{P}_{n-1},\mathbf{P}_n,v_n,T_{\mathrm{p,n}},\Theta_n(k))\,\big|\,n,k\in\mathbb{N}\big\}$, where $\Theta_n(k)=(\alpha_n(k),\beta_n(k),\gamma_n(k))$ determines the orientation of device at time instance k. The ORWP is outlined in the Algorithm 1.

IV. Simulation Results

In the simulation setup, we consider a room of size 10×10 m^2. The user's movement is based on the ORWP mobility model. Fig. 4 shows the PDF and ACF of β for walking and static users with $N=10^4$ realizations. As it can be seen from Fig. 4a and Fig. 4c, the PDF of β follows a Gaussian distribution with a mean value of 28.80 and standard deviation of 3.25 for walking users while it follows a Laplace distribution with $\mu_\beta=30$ and $\sigma_\beta=2.39$ for static users. The

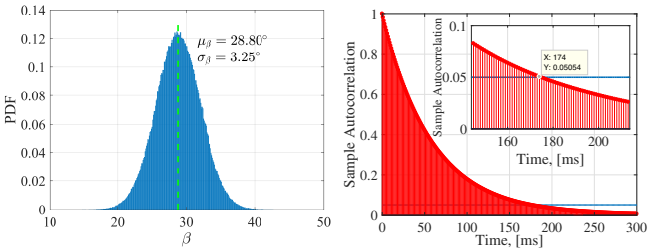

(a) PDF of β for walking users (b) ACF of β for walking users

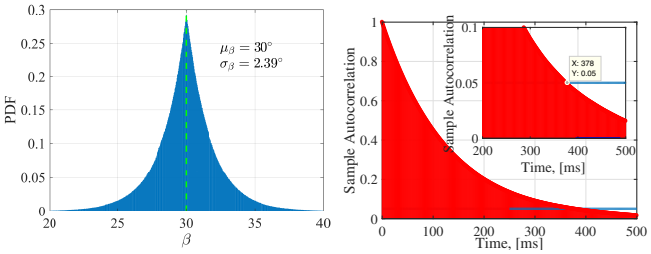

(c) PDF of β for static users (d) ACF of β for static users

Fig. 4: Statistics of β.

average coherence time of β for walking and static users are shown in Fig. 4b and Fig. 4d, respectively. We note that for some realizations the coherence time might be less and for some other realizations, it might be higher than the average coherence time. This effect has been seen in the experimental measurements as well. However, by taking the average values, we find that both of them are very close. By comparing the values of mean, standard deviation and coherence time obtained from Monte-Carlo simulations with the experimental measurements, reported in Table I, the accuracy of the models described in Section III-A and Section III-B is justified.

Next, we investigate the effect of the ORWP mobility model on the handover rate in a LiFi network as a case study. It is noted that similarly the impact of the ORWP model can be evaluated in a mmWave or Terahertz network. Also, instead of handover rate which is one of the key metrics in cellular network design, other parameters such as received signal-to-noise ratio (SNR), user throughput and so on can be considered. Handover rate is defined as [23]:

$$\mathcal{H}=\frac{\sum_{i=1}^{N}N_{\mathrm{h},i}}{\sum_{i=1}^{N}T_{\mathrm{e},i}},\tag{11}$$

where $N_{\mathrm{h},i}$ is the number of handovers during the ith elapsed time, $T_{\mathrm{e},i}$. In fact, the numerator and denominator of (11) denote the total number of handovers and the overall simulation time, respectively.

In this simulation setup, four LiFi APs are assumed such that the network area is divided into four separate quadrants (attocells) with one AP at the center of each attocell. Simulation parameters are presented in Table II. The UE is assumed to be initially connected to the corresponding AP denoted as AP$_j$ for $j=1,2,3,4$. Fig. 5 represents the Monte-Carlo simulations of handover rate for ORWP (shown by the solid line) and conventional RWP (shown by the dashed

TABLE I: Statistics of orientation measurement.

	Static			Walking		
	α	β	γ	α	β	γ
Mean	Ω-90	$\mathcal{U}(20, 40)$	-0.84	Ω-90	28.81	-1.35
Standard deviation	3.67	2.39	2.21	10	3.26	5.42
Coherence Time	0.342	0.377	0.331	0.131	0.176	0.142

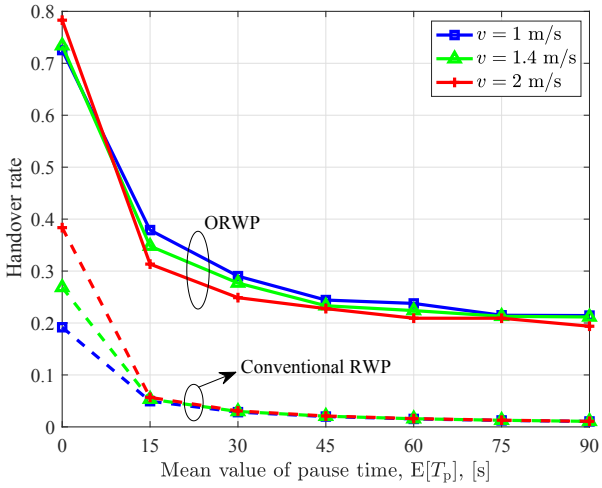

Fig. 5: Handover rate versus mean value of pause time.

TABLE II: Simulation parameters

Parameter	Symbol	Value
Room area	-	10×10 m^2
Locations of APs	-	$(\pm 2.5, \pm 2.5)$
Vertical distance of UE and AP	h	2.15 m
LED half-intensity angle	$\Phi_{1/2}$	60°
Receiver FOV	Ψ_c	90°
Physical area of a PD	A_{PD}	1 cm^2
Gain of optical filter	g_f	1
Refractive index	ς	1

lines) mobility models. In the conventional RWP model, the UE is vertically upward without any random orientation. In the simulations, we assumed that the pause time is chosen from an exponential distribution with the mean value of $\mathbb{E}[T_p]$ seconds [5]. During a pause time, WSS RPs of β are generated for a random period taken from an exponential distribution of $\text{Exp}(1/30)$. The mean values $\overline{\beta}_i$ are chosen uniformly between 20 and 40. Three speed values of $v = 1$ m/s, $v = 1.4$ m/s and $v = 2$ m/s are chosen around the average human walking speed [24]. As can be seen from Fig. 5, the handover rate decreases overall with an increase in the mean value of pause time. The results show a considerable gap between the conventional RWP and the proposed ORWP mobility models, which signifies the difference of these two methods.

Fig. 6 presents the impact of different parameters of correlated Laplace RP β on the handover rate. In these results, we set $v = 1$ m/s. As described in Section III-B, a WSS RP with mean value of $\overline{\beta}_i \sim \mathcal{U}(\beta_{\min}, \beta_{\max})$ is generated for a duration of T_i, where $T_i \sim \text{Exp}(1/\text{T}_\text{m})$. Fig. 6a shows the handover rate versus the expected duration T_m for which $\overline{\beta}_i \sim \mathcal{U}(20, 40)$. A slight decrease of handover rate is observed as T_m increases. The results are illustrated for three values of $\mathbb{E}[T_p]$. As expected, higher handover rate corresponds to lower $\mathbb{E}[T_p]$. Fig. 6b presents the handover rate versus $\mathbb{E}[T_p]$

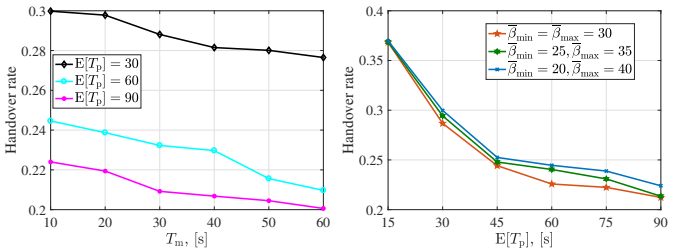

(a) (b)

Fig. 6: Impact of parameters variations of correlated Laplace RP β on handover rate.

for different values of $\beta_{\min}$ and $\beta_{\max}$. For these results, we set $T_\text{m} = 10$. It is noted that the lower handover rate is related to the case of $\beta_{\min} = \beta_{\max}$ which is intuitively true. This is because all $\overline{\beta}_i$'s are the same and the RP β is stationary during the whole time. However, as $\beta_{\min}$ and $\beta_{\max}$ diverge from each other, the handover rate increases. That is, the RP β becomes a non-stationary process.

V. Conclusions

In this study, an extended ORWP mobility model is proposed, in which the orientation of UEs is considered. Inspired by the experimental measurements, we presented a new scheme that takes into account the pause time by generating non-stationary Laplace RP for device orientation. Both correlated Laplace and Gaussian RPs are modeled based on AR(1) for which the parameters are obtained according to the experimental measurements. The accuracy of AR(1) model is validated through Mote-Carlo simulations. Finally, the proposed ORWP mobility model is compared with the conventional RWP in a LiFi cellular network to assess the handover rate. The results confirm the importance of incorporating the random orientation with user mobility to provide a more realistic framework for performance analysis.

Acknowledgment

The authors acknowledge financial support from Engineering and Physical Sciences Research Council (EPSRC) under grant EP/S016570/1 'Terabit Bidirectional Multi-User Optical Wireless System (TOWS) for 6G LiFi'. Prof. Harald Haas acknowledges financial support from the EPSRC under the Established Career Fellowship grant EP/R007101/1 as well as the Wolfson Foundation and the Royal Society.

Appendix

Proof of Lemma 1

As mentioned, the nth sample of correlated Laplace process, ϑ, can be expressed as:

$$\vartheta[n] = \mathrm{Re}\left\{\vartheta_1[n]\vartheta_2[n]\right\} + b_0. \tag{12}$$

For simplicity of notation, we drop the time index n from equations. The mean value of the RP ϑ is given as:

$$\mathbb{E}\left[\vartheta\right] = \mathbb{E}\left[\mathrm{Re}\left\{\vartheta_1\vartheta_2\right\}\right] + b_0. \tag{13}$$

Since ϑ_1 and ϑ_2 are zero-mean RPs, $\vartheta_1\vartheta_2$ is also a zero-mean RP. Hence, $\mathbb{E}\left[\mathrm{Re}\left\{\vartheta_1\vartheta_2\right\}\right] = 0$, and we have $\mathbb{E}\left[\vartheta\right] = b_0$.

Substituting $\vartheta_1 = \vartheta_1^{\mathrm{R}} + j\vartheta_1^{\mathrm{I}}$ and $\vartheta_2 = \vartheta_2^{\mathrm{R}} + j\vartheta_2^{\mathrm{I}}$ in (12), and noting that random variables ϑ_1^{R}, ϑ_2^{R}, ϑ_1^{I} and ϑ_2^{I} are independent, the variance of the random variable ϑ can be obtained as:

$$\sigma_\vartheta^2 = \mathbb{E}\left[\left(\vartheta_1^{\mathrm{R}}\vartheta_2^{\mathrm{R}} - \vartheta_1^{\mathrm{I}}\vartheta_2^{\mathrm{I}}\right)^2\right] - \mathbb{E}^2\left[\vartheta_1^{\mathrm{R}}\vartheta_2^{\mathrm{R}} - \vartheta_1^{\mathrm{I}}\vartheta_2^{\mathrm{I}}\right]. \tag{14}$$

After some simplifications, we arrive at:

$$\sigma_\vartheta^2 = \mathbb{E}\left[\left(\vartheta_1^{\mathrm{R}}\right)^2\right]\mathbb{E}\left[\left(\vartheta_2^{\mathrm{R}}\right)^2\right] + \mathbb{E}\left[\left(\vartheta_1^{\mathrm{I}}\right)^2\right]\mathbb{E}\left[\left(\vartheta_2^{\mathrm{I}}\right)^2\right]. \tag{15}$$

Note that we have:

$$\mathbb{E}\left[\left(\vartheta_i^{\mathrm{R}}\right)^2\right] = \mathbb{E}\left[\left(\vartheta_i^{\mathrm{I}}\right)^2\right] = \frac{\sigma_w^2/2}{1-c_1^2}. \tag{16}$$

Therefore, substituting (16) into (15), we get:

$$\sigma_\vartheta^2 = \frac{\sigma_w^4}{2(1-c_1^2)^2}. \tag{17}$$

The definition of normalized autocorrelation for a WSS RP is [25]:

$$\mathcal{R}_\vartheta(\ell) = \frac{\mathbb{E}[(\vartheta[n]-\mu_\vartheta)(\vartheta[n+\ell]-\mu_\vartheta)]}{\sigma_\vartheta^2}, \tag{18}$$

where $\mu_\vartheta = \mathbb{E}[\vartheta] = b_0$. Substituting for $\vartheta[n] = \mathrm{Re}\left\{\vartheta_1[n]\vartheta_2[n]\right\} + b_0$, (18) can be simplified as:

$$\begin{aligned}
\mathcal{R}_\vartheta(\ell) &= \frac{1}{\sigma_\vartheta^2}\mathbb{E}\left[\mathrm{Re}\left\{\vartheta_1[n]\vartheta_2[n]\right\}\mathrm{Re}\left\{\vartheta_1[n+\ell]\vartheta_2[n+\ell]\right\}\right] \\
&= \frac{1}{\sigma_\vartheta^2}\mathbb{E}\left[\left(\vartheta_1^{\mathrm{R}}[n]\vartheta_2^{\mathrm{R}}[n] - \vartheta_1^{\mathrm{I}}[n]\vartheta_2^{\mathrm{I}}[n]\right)\times\right. \\
&\qquad \left.\left(\vartheta_1^{\mathrm{R}}[n+\ell]\vartheta_2^{\mathrm{R}}[n+\ell] - \vartheta_1^{\mathrm{I}}[n+\ell]\vartheta_2^{\mathrm{I}}[n+\ell]\right)\right] \\
&= \frac{1}{\sigma_\vartheta^2}\mathbb{E}\left[\vartheta_1^{\mathrm{R}}[n]\vartheta_1^{\mathrm{R}}[n+\ell]\vartheta_2^{\mathrm{R}}[n]\vartheta_2^{\mathrm{R}}[n+\ell]\right] \\
&\quad + \frac{1}{\sigma_\vartheta^2}\mathbb{E}\left[\vartheta_1^{\mathrm{I}}[n]\vartheta_1^{\mathrm{I}}[n+\ell]\vartheta_2^{\mathrm{I}}[n]\vartheta_2^{\mathrm{I}}[n+\ell]\right].
\end{aligned} \tag{19}$$

The third equality in (19) is a result of the fact that ϑ_i^{R} and ϑ_i^{I} are independent and identically distributed (i.i.d.) RPs. Substituting $\mathbb{E}\left[\vartheta_i^{\mathrm{R}}[n]\vartheta_i^{\mathrm{R}}[n+\ell]\right] = \sigma_{\vartheta_i^{\mathrm{R}}}^2\mathcal{R}_{\vartheta_i^{\mathrm{R}}}(\ell)$ and similarly for imaginary part in (19), we have:

$$\mathcal{R}_\vartheta(\ell) = \frac{1}{\sigma_\vartheta^2}\left[\sigma_{\vartheta_1^{\mathrm{R}}}^2\sigma_{\vartheta_2^{\mathrm{R}}}^2\mathcal{R}_{\vartheta_1^{\mathrm{R}}}(\ell)\mathcal{R}_{\vartheta_2^{\mathrm{R}}}(\ell) + \sigma_{\vartheta_1^{\mathrm{I}}}^2\sigma_{\vartheta_2^{\mathrm{I}}}^2\mathcal{R}_{\vartheta_1^{\mathrm{I}}}(\ell)\mathcal{R}_{\vartheta_2^{\mathrm{I}}}(\ell)\right] \tag{20}$$

Comparing (16) and (17), we have:

$$\sigma_\vartheta^2 = 2\sigma_{\vartheta_i^{\mathrm{R}}}^4 = 2\sigma_{\vartheta_i^{\mathrm{I}}}^4, \qquad i = 1, 2. \tag{21}$$

Substitution (21) into (20) and noting that $\mathcal{R}_{\vartheta_i^{\mathrm{R}}}(\ell) = \mathcal{R}_{\vartheta_i^{\mathrm{I}}}(\ell) = c_1^\ell$, we have:

$$\mathcal{R}_\vartheta(\ell) = c_1^{2\ell}. \tag{22}$$

This completes the proof of (7).

REFERENCES

[1] M. K. Samimi and T. S. Rappaport, "3-D millimeter-wave statistical channel model for 5G wireless system design," *IEEE Trans. Microw. Theory Tech.*, vol. 64, no. 7, pp. 2207–2225, July 2016.

[2] S. Priebe and T. Kurner, "Stochastic modeling of THz indoor radio channels," *IEEE Trans. Wireless Commun.*, vol. 12, no. 9, pp. 4445–4455, September 2013.

[3] H. Haas, L. Yin, Y. Wang, and C. Chen, "What is LiFi?" *J. Lightw. Technol.*, vol. 34, no. 6, pp. 1533–1544, 2016.

[4] "Cisco Visual Networking Index: Global Mobile Data Traffic Forecast Update, 2017–2022," White Paper, Cisco, Feb. 2019.

[5] C. Bettstetter, H. Hartenstein, and X. Perez-Costa, "Stochastic Properties of the Random Waypoint Mobility Model," *ACM Wireless Netw.*, vol. 10, no. 5, pp. 555–567, Sep. 2004.

[6] X. Lin, R. K. Ganti, P. J. Fleming, and J. G. Andrews, "Towards Understanding the Fundamentals of Mobility in Cellular Networks," *IEEE Trans. Wireless Commun.*, vol. 12, no. 4, pp. 1686–1698, April 2013.

[7] E. Hyytiä and J. Virtamo, "Random Waypoint Mobility Model in Cellular Networks," *Wireless Networks*, vol. 13, no. 2, pp. 177–188, 2007.

[8] C. Bettstetter, G. Resta, and P. Santi, "The Node Distribution of the Random Waypoint Mobility Model for Wireless Ad Hoc Networks," *IEEE Trans. Mobile Comput.*, vol. 2, no. 3, pp. 257–269, July 2003.

[9] E. Hyytia, P. Lassila, and J. Virtamo, "Spatial Node Distribution of the Random Waypoint Mobility Model with Applications," *IEEE Trans. Mobile Comput.*, vol. 5, no. 6, pp. 680–694, June 2006.

[10] M. D. Soltani *et al.*, "Modeling the Random Orientation of Mobile Devices: Measurement, Analysis and LiFi Use Case," *IEEE Trans. Commun.*, vol. 67, no. 3, pp. 2157–2172, Mar. 2019.

[11] Z. Zeng *et al.*, "Orientation Model of Mobile Device for Indoor VLC and Millimetre Wave Systems," in *IEEE 88th Veh. Technol. Conf.(VTC Fall)*, Chicago, IL, USA, Aug 2018, pp. 1–6.

[12] A. A. Purwita *et al.*, "Impact of Terminal Orientation on Performance in LiFi Systems," in *2018 IEEE Wireless Communications and Networking Conference (WCNC)*, Barcelona, Spain, April 2018.

[13] M. D. Soltani *et al.*, "Bidirectional Optical Spatial Modulation for Mobile Users: Toward a Practical Design for LiFi Systems," *IEEE J. Sel. Areas Commun.*, vol. 37, no. 9, pp. 2069–2086, Sep. 2019.

[14] A. A. Purwita, M. D. Soltani, M. Safari, and H. Haas, "Terminal Orientation in OFDM-based LiFi Systems," *IEEE Trans. Wireless Commun.*, vol. 18, no. 8, pp. 4003–4016, Aug. 2019.

[15] I. Tavakkolnia, M. D. Soltani, M. A. Arfaoui, A. Ghrayeb, C. Assi, M. Safari, and H. Haas, "Mimo system with multi-directional receiver in optical wireless communications," in *IEEE International Conference on Communications Workshops (ICC Workshops)*, May 2019, pp. 1–6.

[16] J. M. Kahn and J. R. Barry, "Wireless Infrared Communications," *Proceedings of the IEEE*, vol. 85, no. 2, pp. 265–298, Feb 1997.

[17] M. D. Soltani *et al.*, "Access Point Selection in Li-Fi Cellular Networks with Arbitrary Receiver Orientation," in *Int. Symp. Pers., Indoor Mobile Radio Commun.*, Valencia, Spain, Sept 2016, pp. 1–6.

[18] J. B. Kuipers, *Quaternions and rotation sequences*. Princeton university press Princeton, 1999, vol. 66.

[19] G. E. P. Box and G. Jenkins, *Time series analysis: forecasting and control*. John Wiley & Sons, 2015.

[20] W. J. Szajnowski, "Generation of A Discrete-Time Correlated Laplacian Process," *IEEE Signal Processing Letters*, vol. 7, no. 3, pp. 69–70, March 2000.

[21] T. Ghirmai, "Generating Laplace Process with Desired Autocorrelation from Gaussian AR Processes," in *2015 IEEE Signal Processing and Signal Processing Education Workshop (SP/SPE)*, Snowbird, USA, Aug 2015, pp. 113–117.

[22] D. Tse and P. Viswanath, *Fundamentals of wireless communication*. Cambridge university press, 2005.

[23] M. D. Soltani *et al.*, "Handover Modeling for Indoor Li-Fi Cellular Networks: The Effects of Receiver Mobility and Rotation," in *2017 IEEE Wireless Communications and Networking Conference (WCNC)*, San Fransisco, USA, March 2017, pp. 1–6.

[24] R. W. Bohannon, "Comfortable and Maximum Walking Speed of Adults Aged 20–79 Years: Reference Values and Determinants," *Age and ageing*, vol. 26, no. 1, pp. 15–19, 1997.

[25] K. I. Park, *Fundamentals of Probability and Stochastic Processes with Applications to Communications*. Springer, 2018.